Dalton Transactions

Accepted Manuscript

ROYAL SOCIETY OF CHEMISTRY

www.rsc.org/dalton

Influence of Self-assembly on Intercalative DNA Binding Interaction of Double-chain Surfactant Co(III) Complexes Containing Imidazo[4,5-f][1,10]phenanthroline and Dipyrido[3,2-d:2'-3'-f]quinoxaline ligands: Experimental and Theoretical Study

Karuppiah Nagaraj[a], Gunasekaran Velmurugan[b], Subramanian Sakthinathan[a], Ponnambalam Venuvanalingam[b] and Sankaralingam Arunachalam[a]*

[a,b]*School of Chemistry, Bharathidasan University, Tiruchirappalli-620 024, India.*

A new class of surfactant Co(III) complexes, cis-$[Co(ip)_2(C_{12}H_{25}NH_2)_2](ClO_4)_3$ **(1)** and cis-$[Co(dpq)_2(C_{12}H_{25}NH_2)_2](ClO_4)_3$ **(2)** (ip = imidazo[4,5-f][1,10]phenanthroline, dpq = dipyrido[3,2-d:2'-3'-f]quinoxaline), have been synthesized and characterized by various spectroscopic and physico-chemical techniques. The critical micelle concentration (CMC) values of these complexes in aqueous solution were obtained from conductance measurements. The specific conductivity data (at 303, 308, 313, 318 and 323K) served for the evaluation of the temperature-dependent CMC and the thermodynamics of micellization (ΔG^0_m, ΔH^0_m and ΔS^0_m). The trend in DNA-binding affinities and the spectral properties of a series of complexes, cis-$[Co(ip)_2(C_{12}H_{25}NH_2)_2](ClO_4)_3$ **(1)** and cis-$[Co(dpq)_2(C_{12}H_{25}NH_2)_2](ClO_4)_3$ **(2),** have been experimentally and theoretically investigated. The experimental results indicate that the size and shape of the intercalated ligand and hydrophobicity of the complexes have a marked effect on the binding affinity of complexes to CT DNA in intercalation mode, and the order of their intrinsic DNA-binding constants K_b is K_b**(1)** < K_b**(2).** In addition, the influence of the extended aromatic ring and optical properties of the complexes can be reasonably explained by applying the DFT calculations. The energy gap between HOMO and LUMO indicates that these complexes are prone to interact with CT DNA. Further, molecular docking calculations have also been performed to understand the nature of binding of the complexes and the result confirms that the complexes interact with CT DNA through the alkyl chain. The cytotoxic activity of these complexes on human liver carcinoma cancer cells were determined adopting MTT assay and specific staining techniques, which revealed that the viability of the cells, thus treated was

significantly decreased and the cells succumbed to apoptosis as seen in the changes in the nuclear morphology and cytoplasmic features.

*Corresponding author: S. Arunachalam; Phone: 91-431-2407053; Fax: 91 431 2407043/ 2407045; E-mail: arunasurf@yahoo.com

Introduction

The understanding of the physical nature of DNA cationic surfactant interaction has primary importance due to its significance in biomedical applications, particularly as efficient gene delivery vectors [1]. In cationic detergents between DNA into discrete particles each consisting of a single nucleic acid molecule [2,3], which is released fast into cells with accompanying decondensation. This interesting feature of DNA-surfactant interaction has prompted biophysical characterization of complexes of large DNA molecules with various surfactants [4,5]. Many factors are reported to affect efficient gene transfection including the type of nanoscale structure and the surface charge of DNA/surfactant complex. It is realized that strong DNA/cationic surfactant interaction can help to compact DNA, yielding complexes of small size [6-9]. The cooperative binding of cationic surfactants on DNA chains is primarily driven by both electrostatic attraction and hydrophobic effect. The cationic surfactant can be varied by the molecular structures including conventional single-tailed surfactants [10], Gemini surfactants [11], double-tailed surfactants [12], etc.

The mode of action of many drugs in clinical use for the treatment of cancer, genetic disorders, and viral diseases is believed to be based on their binding to nucleic acids and subsequent modification of the genetic material [13]. Ribonucleic acid (RNA) also plays essential role in normal biological process as well as in the progression of many diseases that led to growing interests in exploiting in designing of a new class of therapeutics [14-16]. A number of small organic molecules are endowed with cytotoxic properties that are exerted through highly specific but non-covalent and reversible interactions with nucleic acid structures [17,18]. The non-covalent interactions are further classified in terms of intercalation and groove binding. Intercalation occurs when planar aromatic molecules are sandwiched between two adjacent base

pairs of nucleic acids. Non-intercalative binding occurs in the major or minor grooves of nucleic acids without inserting any part of the binding molecule between base pairs. The physical and molecular basis of binding of natural alkaloids to nucleic acids has been a subject of extensive study in the recent past [19-21]. The intercalating ligands constitute one of the most widely studied groups as they form important class of compounds for cancer therapy [22]. We have been interested in the synthesis and micelle forming properties of Co(III)/cu(II) complexes containing lipophilic ligands [23-33]. As in biology, such compounds may exhibit novel physical and chemical properties with interesting and useful associated applications. In metal-based drugs, the metal can coordinate ligands in a precise three-dimensional configuration, thus allowing the tailoring of the molecule to recognize and interact with a specific molecular target [34-36]. This is further enhanced by different chemical modifications of ligands. Moreover, metal complexes easily undergo redox reactions and ligand substitution which allow them to participate in biological redox chemistry and interact with biological molecules. It is remarkable that investigations in this area are focused on the use of biologically active complexes formed by essential ions, such as Co (III). In spite of the great effort and success in the study of surfactant Co(III) complexes, such complexes still attract much attention due to the relative simplicity of their synthesis and their interesting properties. Co(III) complexes of bipyridine and phenanthroline chelators are of great interest since they exhibit numerous biological properties such as antitumor, anticandida and antibacterial activity [37-39]. In order to guide the design and synthesis of new complexes with excellent bioactivity, some important factors affecting DNA binding affinities of such a kind of polypyridyl complexes, e.g., the planarity and substituted phenanthroline properties of the intercalative ligands, as well as ancillary ligand effects, have been experimentally summarized in certain scale [40,41a]. In addition to the experimental studies, the transition metal polypyridyl complexes have also attracted many theoretical chemists. Various theoretical researchers have been trying to correlate some theoretical predictions to the experimental findings [41b and 41c].

In this paper, we report two surfactant Co(III) complexes, cis-$[Co(ip)_2(C_{12}H_{25}NH_2)_2](ClO_4)_3$ **(1)** and cis-$[Co(dpq)_2(C_{12}H_{25}NH_2)_2](ClO_4)_3$ **(2)** are synthesized and characterized (Scheme 1 and 2). The trend in DNA-binding affinities and the spectral properties of a series of surfactant Co(III) polypyridyl complexes were experimentally and theoretically studied. The DNA binding constants K_b of the complexes were determined

systematically with spectrophotometric titration. DFT calculations were performed to rationally explain the binding trend and the molecular docking studies carried out to obtain detailed binding information of the complexes with CT DNA. This paper is mainly focused on experimentally revealing the trend in DNA binding affinities of such a type of surfactant Co(III) polypyridyl complexes and on theoretically attempting to understand them in order to effectively control the DNA binding affinities of the complexes by selecting some suitable modified phenanthrolne ligands. This structural feature offers the chance for them to be a candidate for DNA-binding reagents. The cytotoxicty of these surfactant Co(III) complexes against human liver carcinoma cancer cells are also reported.

Results and discussion

Critical micelle concentration (CMC) and thermodynamics of micellization

The specific conductivity of the surfactant Co(III) complexes increases with the complex concentration and temperature. When plots are made of [complex] versus specific conductivity, the slope is reduced after a particular value of concentration. This particular value of concentration at which slope of the plot changes shows micellization and this concentration is chosen as CMC. Fig. 1 and SI (Supplementary Information) Fig. 1 illustrates that the plot for the complexes **(1)** and **(2)**. It was observed that the CMC values increased with increase in the temperature for a given system. This behavior may be related to two competitive effects. First, an increase in temperature causes a decrease in hydration in the hydrophilic group, which favors micellization. Second, an increase in temperature also disrupts the water surrounding the hydrophobic group, and this retards micellization. The relative magnitude of these two opposing effects will determine CMC behavior. The study of CMC versus temperature is often undertaken to obtain information on hydrophobic and head group interactions. This involves deriving various thermodynamic parameters of micelle formation [56-61]. The thermodynamic parameters of micellization for the surfactant Co(III) complexes are presented in Tables 1 and SI Table 1. The observed more negative Gibbs free energy of micellization indicates more favored micellization for the system under study. Moreover, since the changes of CMC with temperature are small, the value of ΔH^0_m and ΔS^0_m must be rather inaccurate and should be considered as

only approximate. As mentioned in our previous reports [23,25,28,29,31], the CMC values for surfactant Co(III) complexes in the present study were also very low compared to those of the simple organic surfactants. Thus it is suggested that our metal surfactant complexes have more capacity to associate themselves forming aggregates than the ordinary synthetic organic surfactants. Moreover, introduction of a metal complex to the hydrophilic part of the amphiphile can remarkably enhance the ability of aggregation.

DNA binding studies

Electronic absorption spectral studies

Titration with UV spectroscopy is an effective method to examine the binding mode of nucleic acid with metal complexes since the observed changes of the spectra may give evidence of the existing interaction mode [62]. Thus, in order to provide evidence for the possibility of binding of complexes to DNA, spectroscopic titration of the solutions of the surfactant Co(III) complexs with DNA has been performed. The UV spectra have been recorded for a constant DNA concentration in different [compound/DNA] mixing ratios (r) and are shown in Fig. 2 and 3 and SI Fig. 3 and 4. As seen from the Figures. 2,3 and SI Figurs 3,4 with the increase of the concentration of CT DNA, the absorption spectrum of surfactant Co(III) complex **(1)** shows hypochromism 28% for below CMC and 31% for above CMC and complex **(2)** shows hypochromism 34% for below CMC and 37% for above CMC with slight red shift on the addition of increasing amounts of DNA. Hypochromism is suggested to arise due to an intercalative mode of binding involving a strong stacking interaction between extending aromaticity of ligand and the base pairs of DNA [63]. Also Co(III) complex containing long aliphatic chain enhances hydrophobic interaction strongly with intercalating the base pairs of DNA. The observed spectroscopic changes are thus, consistent with intercalation of complexes into the DNA base stacks. In order to further elucidate quantitatively the affinity of the surfactant Co(III) complex to CT-DNA, the intrinsic binding constant, K_b has been determined using the equation [64],

$$[DNA]/ (\varepsilon_a-\varepsilon_f) = [DNA]/(\varepsilon_0-\varepsilon_f)+1/K_b(\varepsilon_0-\varepsilon_f)$$

where, [DNA] is the concentration of DNA expressed in base pairs ; ε_a, ε_f and ε_0 are the apparent, free and fully bound Co(III) complex extinction coefficients. A plot of [DNA]/ (ε_a-ε_f) versus [DNA] gives K_b as the ratio of the slope to intercept.

The K_b values of the surfactant Co(III) complexes with CT DNA are given in Table 2. In complex **(1),** which contains ip ligand, that is expected to be planar and possesses a smaller π system than dpq, intercalation is lower [65-68]. Since the complex **(2),** contains dpq ligand (2.4×10^6 M^{-1} for below CMC and 3.1×10^6 M^{-1} for above CMC), it would provide an aromatic moiety extending from the metal center through which overlapping would occur with the base pairs of DNA by intercalation. Besides the binding constant at below CMC values are lower than that at above the CMC values. Above cmc value the surfactant complex presents as both monomers as well as micelles. Aggregation of complex molecules into micelles would reduce their ability to bind to DNA. So there is a difference in K_b values at above cmc and below cmc values. Also the K_b of surfactant Co(III) complexes is very much higher than that for the ordinary metal complexes, like $[Co(bpy)_3]^{3+}$ (K_b, 9.3×10^3 M^{-1}) [69], $[Co(bpy)_2(imp)]^{3+}$ (K_b, 1.1×10^4 M^{-1}) [70], $[Co(bpy)_3(BHBMe)]^{2+}$ (K_b, 1.23×10^4 M^{-1}), $[Co(bpy)_2(BHBNO_2)]^{2+}$ (K_b, 2.06×10^4 M^{-1}) [71], $[Co(ip)_2Cl_2]Cl$ (K_b, 2.9×10^3 M^{-1}), $[Co(dpq)_2Cl_2]Cl$ (K_b, 6.4×10^3 M^{-1}) [72]. This implies that this series of the complexes can intercalate between the base pairs of DNA and thus be protected by DNA efficiently, since the hydrophobic environment inside the DNA helix reduces the accessibility of solvent water molecules to the complex and the complex mobility is restricted at the binding site. Such a trend is also in agreement with that in the binding constants (K_b).

Trend in DNA-binding affinities of the complexes and theoretical explanations

As reported in the literature DNA molecule is generally an electron-donor and the intercalated complex is an electron-acceptor and there are π–π stacking interactions in the DNA-binding of these complexes in intercalation mode. Higher HOMO energy of DNA molecule and lower LUMO energy of the complex result in a stronger interaction between DNA and the complex. Kurita and Kobayashi [73-75] have reported a simple calculation model and reported DFT computed results for stacked DNA base-pairs with backbones. It should be a rather reasonable approximation model for DNA, and thus should be useful for such a discussion. The optimized geometries of the complexes **(1)** and **(2)** are given in SI Fig. 4 (SI-Supporting Information). To

gain further insight into the influence of the extended aromatic ring and trend in DNA-binding activities of the complexes the combined molecular orbital energy level graph for complexes **(1)** and **(2)** is given (SI Fig 5). The HOMOs and LUMOs are often used to relate the spectral properties of complexes and provide decisive clues in designing new complexes. Therefore it is essential to identify and understand the nature of various segments of the complex and their individual contributions towards HOMOs and LUMOs. Hence, the contribution of various fragments of the complexes has been analyzed using QMForge Program [76]. The complexes have been segmented into three fragments, namely Co (Cobalt), L1 (equatorial ligand), L2 (alkyl chain) and their corresponding percentage contributions to frontier molecular orbitals are summarized in Table 3.

The complex **(2)** has the lowest band gap (3.07eV) due to the extension of aromatic ring of the L1 destabilizing the HOMO levels. The frontier molecular orbital shows that the HOMO of complex **(1)** and **(2)** is mainly localized on the L2 (93% and 99% respectively). The LUMO of complex **(1),** there is mainly centered on the L1 (85%) whereas in complex **(2)** it is mainly localized on Co (d_{yz} 54%) and L1 (43%). On the other hand, the HOMO-1 to HOMO-3 of complex **(2)** is localized on L2 of the complex. LUMO+1 of the complex **(1)** is mainly composed of 53% Co (d_{yz}) and 45% of L1. However, extension of aromatic ring in the axial position have a direct effect on the orbital energy of HOMO and as the result HOMO of complex **(2)** is more stabilized than that of complex **(1).** The LUMOs are not influenced by this ligand.

The calculated results indicate that the extension of aromatic ring in the axial position can destabilize the energy of HOMO more significantly than those of the LUMO resulting in narrower HOMO-LUMO energy gap. The LUMO of the complexes of **(1)** and **(2)** lie at -6.92eV and -6.86eV respectively, which distribute predominantly on the intercalative ligands. The predominant LUMO population on the intercalative ligands of the complexes should be advantageous to accept the electron from base-pairs of DNA and the trend in the K_b is well correlated with the LUMO energy values of the complexes.

Molecular docking details

The above experimental results show that these surfactant Co(III) complexes bind to DNA in the intercalation mode and the DNA-binding affinities of these complexes increase in the order: **(1)** < **(2).** Obviously, there are subtle but detectable differences occurred in the DNA-binding properties. Such differences may be resulted from the changes of geometric and electronic structures of these complexes (especially the intercalative ligand) due to the different modified phenanthrolne on the intercalative ligand. Although the single crystal structures of these surfactant Co(III) complexes have not been obtained as far, the DFT calculations can give us some important parameters of the geometric structures of these complexes, as well as some useful information on the electronic structures.

To understand the efficiency of a biologically active drug molecule, the knowledge of its binding location in the CT DNA is very essential and significant. Moreover, the docking study further corroborated the existence of interactions between the Co(III) complexes and DNA. Thus the molecular docking calculations were performed and the most probable docked poses are given in Fig. 4. As seen from the Fig. 4 clearly shows that both the complexes could fit well into the CT DNA with a binding site of three base pairs, preferentially involving the G-C residues as revealed by the docked structure. The availability of the extended alkyl chain makes the complex could bind well to the hydrophobic interior of CT DNA. The complex **(2)** interacts with CT DNA through intercalation and gains additional stabilization due to aromatic moiety extending from the metal center. Thus, the complex **(2)** is found to have higher binding affinity than complex **(1).** In both the cases, the surfactant Co(III) complexes holding three base pairs is like A-T, G-C, G-C to the outer surface, i.e., the groove of the CT DNA. Thus, the G-C regions seem to facilitate a better fit of the complexes into the CT DNA. It is interesting to note that the binding energy of complex **(1)** was 12.0 kcal mol^{-1} less than that of complex **(2)** due to the π–π stacking interaction of extending of aromatic moiety. The aromatic ring structure of surfactant Co(III) complex having a long alkyl chain allows for torsional rotation in order to fit into the narrower helical curvature of the CT DNA. This excellently agrees with the outcome of other experiments (binding constant and spectroscopic studies). Thus, our molecular modeling studies throw light on the binding modes by which these complexes interact with CT DNA and complement the experimental observations.

Thermal denaturation studies

The dissociation of a duplex nucleic acid into two single strands results in significant hyperchromism around 260 nm. The binding of a metal complex to a nucleic acid induces a conformational change of the latter to alter so-called denaturation temperatures depending on the strength and mode of interactions between complex and nucleic acid. In the present work the melting curves of CT-DNA in the absence and presence of complex **(1)** and **(2)** are presented in SI Fig. 6. A T_m of CT-DNA in buffer was determined as for surfactant complexes under our experimental conditions (74.0 ± 0.2^0 C). The DNA intrinsic binding constant of the surfactant Co(III) complexes at T_m were calculated by using McGhee's equation (Eq. (4))[77], where T^0_m is the melting temperature of CT-DNA alone, T_m is the melting temperature in the presence of the Co(III) complexes, ΔH_m is the enthalpy of DNA (per base pair), R is the gas constant, K is the DNA-binding constant at T_m, L is the free complex concentration (approximate by the total complex concentration) at T_m, and n is the size of the binding site.

$$1/T^0_m - 1/T_m = (R/\Delta H_m)\,[\ln(1+KL)]^{1/n} \quad (4)$$

By substitution of the required parameters into Eq. (1), K was determined to be 6.68 x 10^5 M^{-1} for the title complex at 85^0C. Only few thermodynamic parameters such as free energy, enthalpy and entropy changes upon binding of metal complexes to DNA have been measured, although there have been many reports on the interaction of metal complexes with DNA. In fact, the thermodynamic parameter of DNA-complex formation is essential for a thorough understanding of driving forces of the binding of metal complexes to DNA [78]. The change of standard enthalpy was determined according to the van't Hoff's equation (Eq. (5)). The changes of standard free energy and standard entropy of the binding of the title complex to DNA were determined according to Eqs. (6) and (7), where K_1 and K_2 are the DNA-binding constants of the complex at the temperatures T_1 and T_2, respectively. ΔG^0_T, ΔH^0, and ΔS^0 are the changes of standard free energy, standard enthalpy, and standard entropy of the binding of the titled complexes to CT-DNA, respectively.

$$\ln(K_1/K_2) = H^0/R\,(T_1-T_2/T_1T_2) \quad (5)$$

$$\Delta G^0_T = -RT \ln K \quad (6)$$

$$\Delta G^0_T = \Delta H^0 - T\Delta S^0 \quad (7)$$

The value of ΔH^0 is derived to be -82.8 k J mol^{-1} by substituting K_1 = 1.17 x 10^6 M^{-1} (T1 = 298K) and K_2 = 6.68 x 10^5 M^{-1} (T_2 = 358K) into Eq. (4). By substituting K_1 = 1.17 x 10^6 M^{-1}(T1 = 298K) and ΔH^0 = -82.8 k J mol^{-1} into Eqs. (5) and (6), $\Delta G^0_{298\ K}$ = -34.6 k J mol^{-1} and ΔS^0 = -16.2 J mol^{-1} K^{-1} at 25^0 C were derived. It is clearly observed from the experimental results that the complex formation for all the cases was spontaneous with similar negative ΔG^0 values. The negative binding free energy suggests that the energy of the complex-DNA adduct is lower than the sum of the energies of the free complex and DNA, and the binding of the titled complexes to CT DNA is favorable at room temperature. The possible explanation of the entropically driven DNA binding of these types of metal complexes has been discussed in details from the viewpoint of molecular interaction by Haq *et al.* [79] and by us earlier. The negative entropy implies that the degree of freedom of the titled complexes and DNA conformation is reduced upon complex-DNA binding. According to the thermodynamic data, interpreted as follows, the model of interaction between a drug and biomolecule can be concluded as [80]: (1) $\Delta H<0$ and $\Delta S<0$, hydrophobic forces; (2) $\Delta H>0$ and $\Delta S>0$, van der Waals interactions and hydrogen bonds; (3) $\Delta H>0$ and $\Delta S<0$, electrostatic interactions [81]. In order to elucidate the interaction of our complex with DNA, the thermodynamic parameters were calculated. When we apply this analysis to the binding of the complex with CT DNA, we find that $\Delta H < 0$ and $\Delta S < 0$. Therefore, intercalations via hydrophobic interactions are probably the main forces in the binding of the investigated complexes to CT DNA. These results provide that these surfactant Co(III) complexes may interacts with CT DNA in an intercalation mode.

Competitive binding between ethidium bromide (EB) and surfactant Co(III) complexes

In order to investigate the mode of binding of the surfactant Co(III) complexes to DNA, the competitive binding experiment using ethidium bromide (2×10^{-5} M) was carried out. Ethidium bromide (EB) is one of the most sensitive fluorescent probes that can bind to DNA [82-83]. The emission spectra of EB bound to DNA in the absence and the presence of the surfactant Co(III) complexes **(1)** and **(2)** are given in Fig. 5 and SI Fig. 8. The addition of these complexes to DNA pretreated with EB caused an appreciable reduction in the emission intensity, indicating that the

replacement of the EB fluorophore by the complex results in a decrease of the binding constant of ethidium bromide to DNA. According to the classical Stern-Volmer equation [84]:

$$I_o/I = 1 + K_{sv}[Q]$$

where I_0 and I are the fluorescence intensities in the absence and the presence of the complex, respectively. K_{sv} is a linear Stern–Volmer constant and r is the ratio of the total concentration of the complex to that of DNA. The fluorescence quenching of EB bound to DNA by the surfactant Co(III) complexes **(1)** and **(2)** are shown in SI Fig. 8. The quenching plots illustrate that the quenching of EB bound to DNA by the surfactant Co(III) complexes are in good agreement with the linear Stern-Volmer equation, which also indicates that the complexes bind to DNA. In the plot of Io/I versus [complex]/[DNA], K_{sv} is given by the ratio of the slope to intercept. The K_{sv} values for our surfactant Co(III) complexes **(1)** and **(2)** are 0.157 and 0.183, respectively. These data suggest that the interaction of surfactant Co(III) complex **(2)** with DNA is stronger than complex **(1),** which is consistent with the spectral results described above.

Electrochemical studies

The electrochemical investigations of metal-DNA interactions can provide a useful complement to spectroscopic methods, e.g., for non-absorbing species, and yield information about interactions with both the reduced and oxidized form of the metal [85]. In general, the electrochemical potential of a small molecule will shift positively when it intercalates into DNA double helix, and it will shift in a negative direction in the case of electrostatic interaction with DNA [86]. The complete scan in the range +1.0 V to -1.5 V of surfactant Co(III) complexes in the absence of DNA shows a cathodic wave at -0.72 V and an anodic wave at 0.01 V for complex **(1)** and a cathodic wave at -0.24 V and an anodic wave at 0.06 V for complex **(2)** (SI Figures 9 and 10). This quasi-reversible wave can be assigned to the couple Co(III)/Co(II). Complexes **(1)** and **(2)** have similar behavior and the corresponding potentials are given in Table 5. The quasi-reversible redox couple Co(II)/Co(III) for each complex in buffer solution has been studied upon addition of CT DNA and the corresponding potentials as well as their positive shifts are given in Table 4. No new redox peaks appeared after the addition of CT DNA to each complex, but the current intensity of all the peaks decreased significantly, suggesting the

existence of an interaction between each complex and CT DNA. The decrease of current intensity can be attributed to an equilibrium mixture of free and DNA bound complex to the electrode surface [86]. For increasing amounts of CT DNA, the cathodic potential E_{pc} for all complexes shows a positive shift. Hence the positive shifts in the CV peak potential of surfactant Co(III) complexes are indicative of intercalation of these complexes into the DNA [86].

Circular Dichroism Studies

CD spectra is a useful technique in diagnosing changes in DNA morphology during drug–DNA interactions as the CD signals are quite sensitive to the mode of DNA interactions with small molecules [87]. The characteristic CD spectra of right-handed B form DNA consist of two bands: a positive band (275 nm) due to the base stacking and a negative band (245 nm) due to the right-handed helicity. The observed changes of CD signals of DNA are usually assigned to the corresponding changes in DNA structure [87]. It is generally accepted that the classical intercalation enhances the base stacking and stabilizes helicity, and thus increases intensities of the both bands, whereas simple groove binding and electrostatic interaction of small molecules show less or no perturbation on the base stacking and helicity bands [88]. In SI Fig. 11, the CD spectrum of CT DNA was monitored in the presence of increasing amounts of complexes **(1)** and **(2).** The positive band showed an increase in molar ellipticity with a red shift of the band maxima when the complex concentration was progressively increased. This increase in intensity with a red shift in positive bands suggests that surfactant Co(III) complexes binds to CT DNA via intercalation.

Viscosity measurements

The binding modes of the surfactant Co(III) complexes were further investigated by viscosity measurements. In the absence of crystallographic structure data, hydrodynamic methods, which are sensitive to increase in DNA length, are regarded as the least ambiguous and the most critical tests of binding in solution [88a]. Optical or photophysical probes generally provide necessary, but not sufficient clues to support an intercalative binding model. Under appropriate conditions

intercalation causes a significant increase in the viscosity of DNA solutions due to the separation of base pairs at intercalation sites and, hence, increase the overall DNA contour length whereas ligands that bind exclusively in the DNA grooves, groove-face or electrostatic interactions typically cause a bend (or kink) in DNA helix reducing its effective length and thereby its viscosity. The effects of the surfactant Co(III) complexes **(1)** and **(2)** on the viscosity of DNA are shown in SI Fig. 12. Upon addition of increasing the amounts of the titled complexes, the relative viscosity of DNA increase steadily. These results suggest that the titled surfactant Co(III) complexes intercalates between the base pairs of DNA, in agreement with the above experimental results.

Cytotoxity Studies

MTT assay

We examined the cytotoxicity of the effects of these surfactant Co(III) complexes on cultured HepG2 liver cancer cells by exposing cells for 24 and 48 h to the medium containing the complex1 at 8.3-74.7μm (10-90μg/mL) and complex 2 at 8.0-72.0μm (10-90μg/mL) concentration. *In vitro* antitumor activity of these compounds was determined according to the percentage of nonviable cells (%NVC) which was calculated by the following equation:

NVC% = [number of NVC/total number of cells] x 100

The results of these experiments are summarized in Table 5. As shown in table increasing the concentration of surfactant Co(III) complexes was accompanied by progressive increase in the NVC %. This is due to the fact that by increasing the concentration of cationic surfactant complexes the adsorption of ions on cell membranes increases, leading to increase in penetration and antitumor activity.

The results of the cytotoxic activity on human tumor cell lines was determined according to the dose values of drug exposure required to reduce survival in the cell lines to 50% (IC_{50}). It should be noted that the action of the complex as antitumor agents is found to be dependent on the type of tumor cell line (HepG2) tested but, as shown from the results, surfactant Co(III) complexes show excellent cytotoxic activity against tumor cell lines (HepG2) and, at very low concentrations, reduces the survival to 50%. This is due to the fact that cobalt complexes have a

capacity to reduce the energy status in tumors as well as to enhance tumor hypoxia [88b and 88c], which also influences their antitumor activities. It may be also concluded that the level of cellular damage inflicted by these complex depends on the nature of their axial ligands. It is known that phenanthroline-containing metal complexes have a wide range of biological activities such as antitumor, antifungal, apoptosis [89,90] and interaction with DNA inhibiting replication, transcription and other nuclear functions and arresting cancer cell proliferation so as to arrest tumor growth. In general, the high selectivity of action by redox-active cobalt complexes upon tumors is due to their specific reactivity [91]. From these results, surfactant Co(III) complexes seems to offer promise due to the high electron affinity of the metal (which increases its ability to bind DNA) and the ready reducibility of the compounds [92].

Fluorescence Microscopic Analysis of apoptotic cell death (AO and EB staining)

AO/EB staining adopting fluorescence microscopy also revealed apoptosis from the perspective of fluorescence. After HepG2 liver cancer cells were exposed to the concentrations of surfactant Co(III) complexes for 24 h. In this study, we used acridine orange/ethidium bromide (AO/EB) double staining assay [93]. Acridine orange is taken up by both viable and nonviable cells and emits green fluorescence if interrelated into double stranded nucleic acid (DNA). Ethidium bromide is taken up only by nonviable cells and emits red fluorescence by intercalation into DNA. We distinguished four types of cells according to the fluorescence emission and the morphological aspect of chromatin condensation in the stained nuclei: (1) viable cells showing light green fluorescing nuclei with highly organized structure; (2) early apoptotic cells having bright green fluorescing nuclei with chromatin condensation and nuclear fragments; (3) late apoptotic cells having orange to red fluorescing nuclei with condensed or fragmented chromatin; and (4) necrotic cells having red fluorescing without chromatin fragmentation. Viable cells have uniform bright green nuclei with organized structure. Apoptotic cells have orange to red nuclei with condensed or fragmented chromatin. Necrotic cells have a uniformly orange to red nuclei with condensed structure (Fig. 6). Our results indicate that surfactant Co(III) complexes induced apoptosis at the concentrations evaluated, in agreement with the cytotoxic results. The results suggest that the complex treatment caused more cells to take to death in HepG2 liver cancer cells.

Apoptosis Detection Hoechst 33342 DNA Staining

It is possible to perform apoptosis detection assay with Hoechst 33342 (Sigma B-2262), but the increase in fluorescence seen in the apoptotic cells may be less dramatic. Hoechst dyes can also be obtained from Molecular Probes. H33342 is a "vital" DNA stain that binds preferentially to A-T base-pairs. The cells require no permeabilization for labeling, but do require physiologic conditions since the dye internalization is an active transport process. This condition typically varies among cell types (Stander *et al.,* 2009). To investigate if HepG2 liver cancer cells were triggered to undergo apoptosis due to the exposure of surfactant Co(III) complexes, morphological changes of apoptosis were performed in the treated cells by Hoechst 33342 staining. Apoptosis is one of the major pathways that lead to the process of cell death. After the cells were treated with IC_{50} concentrations of surfactant Co(III) complexes for 24 and 48 h the cells were observed for cytological changes adopting Hoechst 33342 staining. The observations revealed that the complexes brought about cytological changes such as chromatin fragmentation, binucleation, cytoplasmic vacuolation, nuclear swelling, cytoplasmic blabbing and late apoptosis indication of dot-like chromatin and condensation (Fig. 7) whereas untreated cells did not show such changes. Data collected from the manual counting of cells with normal and abnormal nuclear features. Both apoptotic and necrotic cells increased in dose-dependent manner. These data clearly indicated that higher doses of surfactant Co(III) complexes resulted in remarkable chromatin condensation and nuclear fragmentation in HepG2 liver cancer cells.

Conclusions

In this work the surfactant Co(III) complexes containing polypyridyl ligand has been synthesized and successfully characterized. The cmc values of these surfactant Co(III) complexes are very low showing more capacity to associate themselves, forming aggregates, compared to those of ordinary synthetic organic surfactants. The experimental results indicate that these surfactant Co(III) complexes could binds to CT DNA by intercalative mode and the binding constant of complex **(1)** is smaller than that of complex **(2)**. Computations support this and further it reveals that the intercalative binding between surfactant Co(III) complexes and CT

DNA is due to the presence of extending aromaticity of ligand and a long aliphatic chain of the complexes. Furthermore, it was observed that surfactant Co(III) complex exhibits considerable ability to bind with the G-C-rich sequence of DNA. As the aromatic moiety extending from the metal centre, the binding ability increases. Both the surfactant Co(III) complexes are cytotoxic to human liver carcinoma cancer cells. Therefore, these complexes might prove to be of application in target-based cancer therapy since the mechanism of cell death appears to be essentially apoptosis, but necrosis also is one of the desired endpoints in cancer therapy.

Experimental Section

Materials and methods

All the reagents were of analytical grade (Sigma-Aldrich and Merck). Calf thymus DNA obtained from Sigma-Aldrich, Germany, was used as such. The spectroscopic titration was carried out in the buffer (50 mM NaCl–5 mM Tris–HCl, pH 7.1) at room temperature. A solution of calf thymus DNA in the buffer gave a ratio of UV absorbance ~1.8–1.9:1 at 260 and 280 nm, indicating that the DNA was sufficiently free of protein [38]. Milli-Q water was used to prepare the solutions. The ligands, ip and dpq were synthesized by using previously published procedures [39,40]. The precursor Co(III) complexes, cis-$[Co(LL)_2Cl_2]Cl$ (where LL_2 = ip and dpq) were prepared by a similar method to the previously published reports [41,42]. Absorption spectra were recorded on a UV–Vis Spectrophotometer using cuvettes of 1 cm path length, and emission spectra were recorded on a JASCO FP 770 spectrofluorimeter. FT-IR spectra were recorded on a FT-IR Perkin Elmer spectrophotometer with samples prepared as KBr pellets. ^1H NMR spectra were recorded on a BRUKER 500 MHz Spectrometer using DMSO as solvent. Conductivity studies were carried out on aqueous solutions of the complexes with an Elico conductivity bridge type CM 82 and a dip-type cell with a cell constant of 1.0. The carbon, hydrogen and nitrogen content of the complexes were determined on a CHNS Elemental Analyzer-elementar (Model: Vario EL III) available at Sophisticated Analytical Instrument Facilities (SAIF), Central Electrochemical Research Institute (CECRI) Karaikudi, India. The anticancer studies were carried out at PCBS Research Centre, Pondicherry University.

Synthesis of double chain surfactant Co(III) complexes

Preparation of cis-$[Co(ip)_2(C_{12}H_{25}NH_2)_2](ClO_4)_3$ (1)

To a solution of cis-$[Co(ip)_2Cl_2]Cl$ (0.53 g) dissolved in water (10 mL), dodecylamine (0.26 mL) in ethanol (2 mL) was added dropwise over a period of 30 min. The mixture was set aside at room temperature for 4 days until no further change was observed. Afterwards, a saturated solution of sodium perchlorate in perchloric acid was added. A pasty solid mass separated out slowly and it was filtered off, washed with small amounts of alcohol followed by acetone, and then dried in air. The semi-dried material was further dried over fused calcium chloride in a drying pistol and stored in a vacuum desiccator. UV $\lambda_{max}(CH_2Cl_2)$/nm 248 (π- π^*), 290 (n- π^*), 370 (MLCT). FT-IR (KBr)/ cm^{-1} 786, 725, 1384 (C=N), 2914, 2852, 1104 and 621. ^1H NMR (400 MHz; $CDCl_3$): δ 0.96 (m, 6H, CH_3), 1.29-4.02 (44H, Aliphatic-H), 4.21 (m, 2H, NH_2), 4.41(m, 2H, NH_2), 5.43 (m, 2H, NH), 7.34 (m, 12H, Ar-H), 7.67 (s, 2H, Ar-H). ^{13}C NMR (400 MHz; $CDCl_3$): δ 24.27, 24.30, 29.32, 32.92, 33.12, 34.77, 35.01 (Aliph-C's), 117.83, 118.58, 118.81, 120.92, 127.37, 127.86, 128.35, 129.35, 129.79, 137.17, 138.27, 148.08, 150.08, 160.30, 161.60, 165.37, 165.67 (Ar-C's). Calcd. for $C_{53}H_{78}CoN_{10}$: C, 52.60, H, 6.07, N 11.75. Found: C 51.60, H, 6.30, N, 11.83.

Preparation of cis-$[Co(dpq)_2(C_{12}H_{25}NH_2)_2](ClO_4)_3$ (2)

The cis-$[Co(dpq)_2(C_{12}H_{25}NH_2)_2](ClO_4)_3$ complex was synthesized similar to the procedure described above, except that we have added dpq ligand in the reaction mixture instead of ip ligand. [Caution: Perchlorate salts of metal complexes with organic ligands are potentially explosive. Only small amounts of the material should be prepared and handled with great care]. UV $\lambda_{max}(CH_2Cl_2)$/nm 250 (π- π^*), 293 (n- π^*), 374 (MLCT). FT-IR (KBr)/ cm^{-1} 791, 728, 1386 (C=N), 2912, 2850, 1100 and 620. ^1H NMR (400 MHz; $CDCl_3$): δ 0.98 (m, 6H, CH_3), 1.18-4.31 (44H, Aliphatic-H), 3.72-3.82 (m, 4H, NH_2), 5.43 (m, 2H, NH), 6.5-7.8 (16H, Ar-H). ^{13}C NMR (400 MHz; $CDCl_3$): δ 24.27, 24.30, 29.32, 32.92, 33.12, 34.77, 35.01 (Aliph-C's), 117.83, 118.58, 118.81, 120.92, 127.37, 127.86, 128.35, 129.35, 129.79, 137.17, 138.27, 148.08, 150.08, 160.30, 161.60, 165.37, 165.67 (Ar-C's). Calcd. for $C_{55}H_{78}CoN_{10}$: C, 52.62, H, 6.11, N 11.38. Found: C 52.67, H, 6.17, N, 11.59.

Estimation of amount of Cobalt in Complexes 1 and 2

Cobalt content in the surfactant Co(III) complexes was estimated according to Kitson [47]. Briefly, a known weight of the complex was reduced with tin and concentrated hydrochloric acid. The reduced aqueous cobalt(II) ion was made up to 10 mL in volumetric flask

using 0.1 M perchloric acid. 2 mL of this solution and 1 mL of 50% ammonium thiocyanate solution were pipetted out into a 10 mL volumetric flask and made up to the mark with acetone. The absorbance of this solution was measured at 625 nm against a reagent blank. From the absorbance, the concentration of cobalt was calculated. The percentage of cobalt thus obtained for our surfactant Co(III) complexes is Co 4.98 (4.89) for complex **(1)** and Co 4.88 (4.71) for complex **(2).**

Estimation of critical micelle concentration (CMC) values

The CMC values of the complexes were determined conductometrically using a specific conductivity meter. The conductivity cell was calibrated with KCl solution in the appropriate concentration range. Various concentrations of surfactant Co(III) complexes were prepared in the appropriate range in aqueous solution. The conductivity of these solutions was measured at 303, 308, 313, 318 and 323K. The temperature of the thermostat was maintained constant, to be within ±0.01. The conductance was measured after thorough mixing and temperature equilibration at each dilution. The establishment of equilibrium was checked by taking a series of readings at 15 min intervals until no significant change occurred. At all temperatures a break in the conductance versus concentration in the plots, characteristic of micelle formation, was observed. The CMC values were determined by fitting the data points above and below the break to two equations of the form $y = mx + c$ and solving the two equations simultaneously to obtain the point of intersection. Least-squares analysis was employed, and the correlation coefficients were greater than 0.98 in all the cases.

DNA binding experiments

The DNA concentration per nucleotide was determined adopting absorption spectroscopy using the known molar extinction coefficient value of 6600 M^{-1} cm^{-1} at 260 nm [48]. Absorption titrations were performed by using a fixed surfactant Co(III) complex concentration to which increments of the DNA stock solution were added. Surfactant Co(III) complex–DNA solutions were incubated for 10 min before the absorption spectra were recorded. For fluorescence experiments, DNA was pretreated with ethidium bromide (EB) for 30 min. The surfactant Co(III) complexes were then added to this mixture and the effect on the emission intensity was measured. The samples were excited at 515 nm and emission was observed between 500 and 700 nm. These experiments were carried out in 50 mM NaCl–5 mM Tris–HCl at pH 7.1 in aqueous media. All voltammetric experiments were performed in a single compartment cell with a three-

electrode configuration on a EG&G PAR 273 potentiostat equipped with a personal computer. The working electrode was a glassy carbon and the reference electrode was standard calomel electrode. A platinum wire was used as the counter electrode. The supporting electrolyte was phosphate buffer at pH 7.1. Solutions were deoxygenated by purging with nitrogen gas for 15 min prior to measurements; during measurements a stream of nitrogen gas was passed over the solution. Circular dichroic experiments were recorded on a JASCO J-716 spectropolarimeter (220-320 nm) were obtained at 25^{o}C using a quartz cell of 1cm path length. Each CD spectrum was collected after averaging over at least 4 accumulations using a scan speed of 100 nm min^{-1} and 1s response time. The region between 220nm and 320 nm was scanned for each sample. The spectra was recorded in the absence and in the presence of surfactant Co(III) complexes. Viscosity experiments were carried out using an Ubbelodhe viscometer maintained at a constant temperature of 29.0 ± 0.1^{0}C. Calf thymus DNA (1×10^{-5}M) sample solutions were prepared by sonication in order to minimize complexities arising from DNA flexibility. Data were presented as $(\eta / \eta^{0})^{1/3}$ versus binding ratio, where g is the viscosity of DNA in the presence of the complex, and η^{0} is the viscosity of DNA alone. The relative viscosity was calculated according to the relation $\eta = (t - t_0)/t_0$, where t_0 is the flow time for the buffer and t is the observed flow time for DNA in the presence and absence of the complex [49].

Cytotoxicity assay

The cytotoxicity of the surfactant Co(III) complexes were measured in the MTT (3-(4,5-dimethylthiazol-2-yl)-2,5-diphenyl tetrazolium bromide) assay as described by us earlier [50]. The complexes were first dissolved quantitatively in dimethyl sulfoxide (DMSO, Sigma, USA) to make the stock solution. Briefly, cells were seeded at a density of 5 x 10^4 HepG-2 liver cancer cells/well into 96-well plates. After 24 h, the cells were treated with surfactant cobalt (III) complexes at various concentration (10, 30, 60, 90 µg/ml) and incubated for 24 and 48 hours as indicated. At the end of the incubations, 10µl of 3-(4-5 dimethylthiozol-2-yl) 2-5 diphenyl-tetrazolium bromide (MTT) (5 mg/ml) per well was added and incubated in dark at 37°C for 4 hours. The formazan crystals formed after 4 hours were solubilized in 100µl of DMSO after aspirating the medium. The absorbance was monitored at 570 nm (measurement) and 630 nm using a 96 well plate reader (Bio-Rad, Hercules, CA, USA). The IC_{50} value was defined as the concentration of compound that produced a 50% reduction of cell viability.

Evaluation of apoptosis (Acridine orange and ethidium bromide staining)

Acridine orange and ethidium bromide staining was performed as described by Spector *et al.* [50]. Twenty-five microliters of cell suspension of each sample (both attached, released by trypsinization, and floating), containing 5×10^5 cells, was treated with AO and EB solution (one part of 100 mg/mL AO and one part of 100 mg/mL EO in PBS) and examined under a fluorescent microscope (Carl Zeiss, Germany) using an UV filter (450-490 nm). Three hundred cells per sample were counted in tetraplicates for each dose point. Cells were scored as viable, apoptotic or necrotic as judged by the staining, nuclear morphology and membrane integrity, and percentages of apoptotic and necrotic cells were then calculated. Morphological changes were also observed and photographed. The amount of 200 µL of dye mixture (100 µL/mg AO and 100 µL/mg EB in distilled water) was mixed with 2 mL cell suspension (30,000 cells/mL) in 6-well plate. The suspension was immediately examined and viewed under Olympus inverted fluorescence microscope (Ti-Eclipse). We observed untreated cells as controls and cells treated with testing material IC_{50} concentrations for 24 h of exposure. HepG2 were seeded in a 24-well plate (50,000 cells per well). After 24 h of cells incubation, the medium was replaced with 100 µL medium containing IC_{50} dose of testing material. Untreated cells served as the control. After 24 h, aspirate the media and treat with prepared dye and observe under the fluorescent microscope.

Hoechst 33342 (H342) staining

Stock H342 solution should be originally suspended in dH_2O at a 1mM concentration (H342 will precipitate in PBS). This procedure is very sensitive to cell concentration and pH of the media. Cells should be approximately 1-2x10^6/ml, in buffered media, pH 7.2. It is also helpful to include 2% fetal calf serum to maintain the cells. Add H342 dye from the stock solution to cell suspension to respective final concentration. Cells are then incubated at 37^{o}C for 1 hour. Drug was added and incubated for 24 and 48 hours. Time is a critical factor due to the transport of the dye. Typically, 30 minutes is a minimum, but it is important to remember that the signal may begin to degrade after ~120 minutes. It is recommended that the staining kinetics be

empirically defined. Analyze apoptosis under fluorescent microscope after incubation. Washing is not recommended.

Computational details

Computational studies on the complexes have been performed using HEX 6.3 software which is an interactive molecular graphics program for the interaction, docking calculations, and to identify possible binding site of the biomolecules [51]. The density functional theory (DFT) calculations at B3LYP level were carried out using the GAUSSIAN09 program [52]. The geometries of the complexes under study were optimized using standard 6-31G** basis sets for N, C and H elements and LANL2DZ for Cobalt with effective core pseudo potentials [53]. The coordinates of metal complexes were taken from their optimized structure as a .mol file and were converted to pdb format using GaussView software. The crystal structure of B-DNA (PDB ID: 1BNA) is retrieved from the protein data bank [54]. All possible poses have been considered as starting points and the docking analysis was performed. The default parameters were used for the docking calculation with correlation type shape only, FFT mode at 3D level, grid dimension of 6 with receptor range 180 and ligand range 180 with twist range 360 and distance range. Visualization of the docked systems has been further analyzed with PyMOL software package [55].

Acknowledgments

K. Nagaraj sincerely acknowledges the UGC- COSIST and DST-FIST programmes of the Department of Chemistry, Bharathidasan University for UGC-RFSMS fellowship. Financial assistance from the CSIR (Grant No. 01(2461)/11/EMR-II), DST (Grant No. SR/S1/IC-13/2009) and UGC (Grant No. 41-223/2012(SR) sanctioned to Prof. S. Arunachalam are also gratefully acknowledged. G. V thanks University Grants Commission (UGC), India for the financial support in the form of BSR Meritorious Student Fellowship. P. V thanks Department of Science and Technology (DST), India for Major Research Project (Ref. No: SB/S1/PC-52/2012).

References

1 A. D. Miller, *Angew. Chem. Int. Ed. Eng.,* 1998, **37,** 1768-1785.

2 J. P. Behr, *Tetrahedron Lett.,* 1986, **27,** 5861-5864.

3 S. M. Melnikov, and V. G. Sergeyev, *J. Am. Chem. Soc.,* 1995, **117,** 9951-9956.

4 C. H. Spink, and , J. B. Chaires, *J. Am. Chem. Soc.,* 1997, **119,** 10920-10928.

5 S. M. Melnikov, V. G. Sergeyev, and K. Yoshizava, *J. Am. Chem. Soc.,* 1995, **117,** 2401-2408.

6 S. Marchetti, G. Onori and C. Cametti, *J. Phys. Chem. B* 2005, **109,** 3676-3680.

7 D. Matulis, I. Rouzina and V. A. Bloomfield, *J. Am. Chem. Soc.,* 2002, **124,** 7331-7342

8 R. Dias, S. Melnikov, B. Lindman and M. G. Miguel, *Langmuir* 2000, **16,** 9577-9583.

9 Y. L. Wang, P. L. Dubin and H. W. Zhang, *Langmuir* 2001, **17,** 1670-1673.

10 S. Bhattacharya and P. V. Dileep, *Bioconjugate Chem.,* 2004, **15,** 508-519.

11 A. Bajaj, P. Kondaiah and S. Bhattacharya, *Bioconjugate Chem.,* 2007, **18,** 1537-1546.

12 J. Zhou, K. T Shum, J. C. Burnett and J. J. Rossi, *Pharmaceutical*s 2013, **6,** 85-107. doi:10.3390/ph6010085.

13 M. Kwiat, R. Elnathan, M. Kwak, J. W. de Vries, A. Pevzner, Y. Engel, L. Burstein, A. Khatchtourints, A. Lichtenstein, E. Flaxer, A. Herrmann and F. Patolsky, *J. Am. Chem. Soc.,* 2012, **134,** 280-92.

14 A. M. Pyle, J. P. Rehmann, R. Meshoyrer, C. V. Kumar, N. J. Turro and J. K. Barton, *J. Am. Chem. Soc.,* 1989, **111,** 3051-3058.

15 A. M. Badawi, M. A. S. Mohamed, M. Z. Mohamed and M. M. Khowdairy, *J. Cancer Res.,* 2007, **3,** 198-206.

16 S. Bhattacharya and S. S. Mandal, *Biochim. Biophys. Acta* 1997, **1323,** 29-44.

17 Y. Ni, D. Li and S. Kokot, *Anal. Biochem.,* 2006, **352,** 231-242.

18 J. R. Thomas and P. J. Hergenrother, *Chem. Rev.,* 2008, **108,** 1171-1224.

19 J. Gallego and G. Varani, *Acc. Chem. Res.,* 2001, **34,** 836-843.

20 C. S. Chow and J. K. Barton, *Biochemistry* 1992, **31,** 5423-5429.

21 H. Xu, H. Deng, Q. L. Zhang, Y. Huang, J. Z. Liu and L. N. Ji, *Inorg. Chem. Commun.,* 2003, **6,** 766-768.

22 M. D. M. Ismal, P. Pandya, S. R. Chowdhury, S. Kumar and G. S. Kumar, *J. Mol. Struct.,* 2008, **891,** 498-507.

23 K. Nagaraj and S. Arunachalam, *New J. Chem.* DOI: 10.1039/c3nj00832k

24 K. Nagaraj and S. Arunachalam, *Inter. J. Biol. Macro. Mol.,* 2013, **62,** 273-280.

25 K. Nagaraj and S. Arunachalam, *Aust. J. Chem.,* 2013, **66,** 930-937.

26 K. Nagaraj and S. Arunachalam, J. Biomol. Str. Dyn. (DOI: 10.1080/07391102.2013.879837).

27 K. Nagaraj and S. Arunachalam, *Z. Phys. Chem.,* 2013, **227,** 1-19.

28 K. Nagaraj and S.Arunachalam, *Trans. Met. Chem.,* 2012, **37,** 423-429.

29 K. Nagaraj and S. Arunachalam, *Trans. Met. Chem.,* 2013, **38,** 649-657.

30 K. Nagaraj and S. Arunachalam, *Monatsh. Chem.,* (DOI 10.1007/s00706-013-1080-x).

31 K. Nagaraj and S. Arunachalam, *J. Inclu. Phenom. Macro. Chem.,* (DOI 10.1007/s10847-013-0365-3).

32 K. Nagaraj, S, Sakthinathan and S. Arunachalam, *J. Fluoresence* (DOI 10.1007/s10895-013-1332-5).

33 K. Nagaraj, S. Ambika, S. Rajasri, S. Sakthinathan, S. Arunachalam, *Colloids and Surfaces B: Biointerfaces* 2014, **122,** 151-157

34 D. Gibson, *Dalton Trans.* 2009, 10681-10689.

35 K. J. Davis, J. A. Carrall, B. Lai, J. R. Aldrich-Wright, S. F. Ralpha, C. T. Dillon, *Dalton Trans.* 2012, **41,** 9417-9426.

36 A. Casini, J. Reedijk, *Chem. Sci.* 2012, **3,** 3135-3144.

37 C. Deegan, M. McCann, M. Devereux, B. Coyle, D. A. Egan, *Cancer Lett.* 2007, **247** 224-233.

38 M. McCann, M. Gerghty, M. Devereux, D. O'Shea, J. Mason, L. O'Sullivan, *Met. Based Drugs* 2000, **7**, 185-193.

39 a)Y. Xiong, L. N. Ji, *Coord. Chem. Rev.,* 1999, **711,** 185-186; b) P. Hohenberg and W. Kohn, *Phys. Rev. B,* 1964, **136,** 864-869; c) A. D. Becke, *J. Chem. Phys.,* 1993, **98**, 1372-1377.

40 M. F. Reichmann, S. A. Rice, C. A. Thomas and P. Doty, *J. Am. Chem. Soc.,* 1954, **76,** 3047-3053.

41 Bonnitcha *et al*., *Dalton Trans.* 2012, **41,** 11293-11304.

42 L. N. Ji, X. H. Zou and J. G. Liu, *Coord. Chem. Rev.,* 2001, **513,** 216–217.

43 S. Ghosh, A. C. Barve, A. A. Kumbhar, A. S. Kumbhar, V. G. Puranik, P. A. Datar, U. B. Sonawane and R. R. Joshi, *J. Inorg. Biochem.,* 2006, **100,** 331-343.

44 A. A. Vlcek, *Inorg. Chem.,* 1967, **6,** 1425-1427.

45 J. G. Collins, A. D. Sleeman, J. R. Aldrich-Wright, I. Greguric and T. W. Hambley*, Inorg Chem.,* 1998, **37,** 3133-3141.

46 J. Z. Wu, B. H. Ye, L. Wang, L. N. Ji, J. Y. Zhou, R. H. Li and Z. Y. Zhou, *J. Chem. Soc. Dalton Trans.*, 1997, 1395-1401.

47 R. E. Kitson, *Anal. Chem.,* 1950, **22,** 664–667.

48 J. K. Barton, J. M. Goldberg, C. V. Kumar and N. J. Turro, *J. Am. Chem. Soc.,* 1986, **108,** 2081-2088.

49 M. L. Morris and D. H. Busch, *J. Am. Chem. Soc.,* 1960, **82,** 1521-1524.

50 D. L. Spector, R. D. Goldman and L. A. Leinwand, *Culture and biochemical Analysis of cells, In: Cell: A Laboratory Manual,* vol. 1, Cold Spring Harbor Laboratory Press, Cold Spring Harbor, New York, 1998.

51 J. B. Foresman, A. E. Frisch, *Exploring Chemistry with Electronic Structure Methods,* second ed., Gaussian, Inc., Pittsburgh, PA, 1996.

52 K. Fukui, T. Yonezawa and H. Shingu, *J. Chem. Phys.,* 1952, **20,** 722-725

53 I. Fleming, *Frontier Orbital and Organic Chemical Reaction,* Wiley, New York, 1976.

54 D. Reha, M. Kabelac, F. Ryjacek, J. Sponer, J.E. Sponer, M. Elstner, S. Suhai and P. Hobza, *J. Am. Chem. Soc.,* 2002, **124,** 3366-3376.

55 N. Kurita and K. Kobayashi, *Comput. Chem.,* 2000, **24,** 351-357.

56 L. Jin and P. Yang, *Polyhedron* 1997, **16,** 3395-3398.

57 T. I. A. Gerber, *J. Coord. Chem.,* 2003, **56,** 1397-1407.

58 M. R. Rosenthal, *J. Chem. Educ.,* 1973, **50,** 331-335.

59 J. D. Miller and R. H. Prince, *J. Chem. Soc., A* 1969, 519-520.

60 S. Castellano, H. Gunther and S. Ebersole, *J. Phys. Chem.,* 1965, **69,** 4166-4176.

61 P. C. Griffiths, I. A. Fallis, T. Chuenpratoom and R. Watanesk, *Adv Colloid Int Sci.,* 2006, **122,** 107-117.

62 P. Mukerjee, J. Phys. Chem., 1962, 66, 1375-1376.

63 J. J. Galan, A. Gonzalez-Perez and J. R. Rodriguez, *J. Therm. Anal. Calorim.,* 2003, **72,** 465-470.

64 A. Gonzalez-Perez, J. C. Del Castillo, T. Czapkiewicz and J. R. Rodrigue, *Colloid Polym. Sci.,* 2002, **280,** 503-508.

65 R. Zana, *J. Colloid Interface Sci.,* 1980, **78,** 330-337.

66 R. F. Pasternack, E. J. Gibbs and J. J. Villafranca, *Biochemistry* 1983, **22,** 2406-2414.

67 A. M. Pyle, J. P. Rehmann, R. Meshoyrer, C. V. Kumar, N. J. Turro and J. K. Barton, *J. Am. Chem. Soc.,* 1989, **111,** 3051-3058.

68 M. T. Carter, M. Rodriguez and A. J. Bard, *J. Am. Chem. Soc.,* 1989, **111,** 8901-8911.

69 P. Tamil Selvi, and M. Palaniandavar, *Inorg. Chim. Acta,* 2002, **337,** 420-428.

70 S. Satyanarayana, J. C. Dabroniak and J. B. Chaires, *Biochemistry* 1992, **31,** 9319-9324

71 K. R. Sangeetha Gowda, H. S. Bhoiya Naik, B. Vinay Kumar, C. N. Sudhamani, H. V. Sudeep, T. R. Ravikumar Naik, G. Krishnamurthy, *Spectrochim. Acta A: Mol. Biomol. Spec.* 2013, **105,** 229-37.

72 S. Nehru, S. Arunachalam, R. Arun, K. Premkumar, *J. Biomol. Str. Dyn.* 2014, **32,** 1876-1888.

73 K. Fukui, T. Yonezawa and H. Shingu, *J. Chem. Phys.,* 1952, **20,** 722-725

74 I. Fleming, *Frontier Orbital and Organic Chemical Reaction,* Wiley, New York, 1976.

75 N. Kurita and K. Kobayashi, *Comput. Chem.,* 2000, **24,** 351-357

76 A. L. Tenderholt, *QMForge: A Program to Analyze Quantum Chemistry Calculations,* Version 2.3.2, http://qmforge.sourceforge.net.

77 J. D. McGhee, *Biopolymers* 1976, **15,** 1345-1375

78 M. Gellert, C. Smith, D. Neville and G. Felsenfeld, *J. Mol. Biol.,* 1965, **11,** 445-457.

79 I. Haq, P. Lincoln, D. Suh, B. Norden, B. Z. Chowdhry,J. B. Chaires, *J. Am. Chem. Soc.,* 1995, **117,** 4788-4796.

80 V. A. Izumrudov, M. V. Zhiryakova, A. A. Goulko, *Langmuir* 2002, **18,** 10348-10356.

81 V. A. Izumrudov, M. V. Zhiryakova and S. E. Kudaibergenov, *Biopolymers* 2000, **52,** 94-108.

82 B. C. Baguley and M. LeBret, *Biochemistry* 1984, **23,** 937-943.

83 T. B. Wyman, F. Nicol, O. Zelphati, P. V. Scaria, C. Plank and F. C. Szoka, *Biochemistry* 1997, **36,** 3008-3017.

84 J. R. Lakowicz and G. Webber, *Biochemistry* 1973, **12,** 4161-4170.

85 P. Uma Maheswari, and M. Palaniandavar, *J. Inorg. Biochem.,* 2004, **98,** 219-230.

86 M. T. Carter and A. J. Bard, *J. Am. Chem. Soc.,* 1987, **109,** 7528-7530.

87 L. M. Chen, J. Liu, J. C. Chen, C. P. Tan, S. Shi, K. C. Zheng and L. N. Ji, *J. Inorg. Biochem.,* 2008, **102,** 330-341.

88 S. Satyanaryana, J. C. Daborusak and J. B. Chaires, *Biochemistry* 1993, **32,** 2573-2584; b) J. M. Brown, *Cancer Res* 1999, **59,** 5863-5870; c) B. G. Wouters, S. A. Weppler, M. Koritzinsky, W. Landuyt, S. Nuyts, J. Theys, R. K. Chiu, P. Lambin, *Eur. J Cancer* 2002, **38,** 240-257.

89 B. Coyle, P. Kinsella, M. McCann, M. Devereux, R. O. Connor, M. Clynes, K. Kavanagh, *Induction of apoptosis in yeast and mammalian cells by exposure to 1,10-phenanthroline metal complexes,* Toxicology in Vitro : an International Journal Published in Association With BIBRA 18 (2004) 63-70.

90 B. Coyle, M. McCann, K. Kavanagh, M. Devereux and M. Geraghty, *Biometals* 2003, **16,** 321-329.

91 S. Osinsky, I. Levitin, L. Bubnovskaya, A. Sigan, I. Ganusevich, *Exper. Oncol.* 2004, **26,** 140-144.

92 A. M. Badawi, M. MekawiAS, M. Z. Mohamed, M. M. Khowdairy, *J. Cancer Res. Therapeu.* 2007, **3,** 198-206.

93 D. Baskic, S. Popovic, P. Ristic, N. N. Arsenijevic, *Cell Biology International* 2006, **30,** 924-932.

Scheme captions

Scheme 1. Synthetic procedure of surfactant cobalt(III) complexes

Figure captions

Figure. 1. Electrical conductivity vs. complex **(1)** concentration in aqueous solutions.

Figure. 2. Absorption spectra of complex **(1)** (Above cmc): in the absence (dotted line) and in the presence (solid lines) of increasing amounts of CT DNA. {Inset: Plot of [DNA] / (ε_a-ε_f) vs. [DNA]}. [complex] =1.0 × 10^{-4} M; [DNA] = 0-9.1 × 10^{-5} M.

Figure. 3. Absorption spectra of complex **(1)** (Below cmc): in the absence (dotted line) and in the presence (solid lines) of increasing amounts of CT DNA. {Inset: Plot of [DNA] / (ε_a-ε_f) vs. [DNA]}. [complex] = 1.0×10^{-6} M; [DNA] = 0-9.1×10^{-5} M.

Figure. 4. Docked pose of surfactant Co(III) Complexes bound to the CT DNA: (a) Complex **(1)** with B-DNA (b) Complex **(2)** with B-DNA.

Figure. 5. Emission spectra of EB bound to CT DNA: in the absence and in the presence of surfactant Co(III) complex **(1)**. [EB] = 2×10^{-5} M, [DNA] = 1×10^{-4} M, [Complex] = 0-1.43×10^{-6}

Figure. 6. Photomicrographs of control and AO and EB stained HepG2 liver cancer cells incubated for 24 hours with surfactant Co(III) complexes **(1)** and **(2).** A,B Untreated control cells. C,D surfactant Co(III) complex treated control cells. ; Viable (light green), early apoptotic (bright green fluorescing), late apoptosis (red to orange fluorescing) and necrosis (red fluorescing) cells were observed. Magnification at 20x.

Figure. 7 Surfactant Co(III) complexes **(1)** and **(2)** induces apoptosis in HepG2 liver cancer cells. Representative fluorescent micrographs of HepG2 liver cancer cells stained with Hoechst 33342 fluorescent dye after the compound exposure for 24 and 48 hours. I, II Untreated control cells; A,B,C and, D surfactant Co(III) complex treated control cells. A, C – 24 hours; B, D - 48 hours. Magnifications at 20X.

Table captions

Table 1. CMC values of the surfactant Co(III) complex **(1)** in aqueous solution.

Table 2. The binding constant (K_b) and Stern-Volmer constant (K_{SV}) of surfactant Co(III) complexes **(1)** and **(2)** with CT DNA.

Table 3. Frontier molecular orbital compositions (%) of surfactant Co(III) complexes **(1)** and **(2)** at the B3LYP/LANL2DZ level.

Table 4. Cyclic voltammetric data (mV) of surfactant Co(III) complexes **(1)** and **(2),** a scan rate of 100 mV/s with phosphate buffer as supporting electrolyte.

793 Table 5. IC_{50} by MTT-3-(4-5 dimethylthiozol-2-yl) 2-5 diphenyl-tetrazolium bromide method.

794

795 **Schemes**

796

797

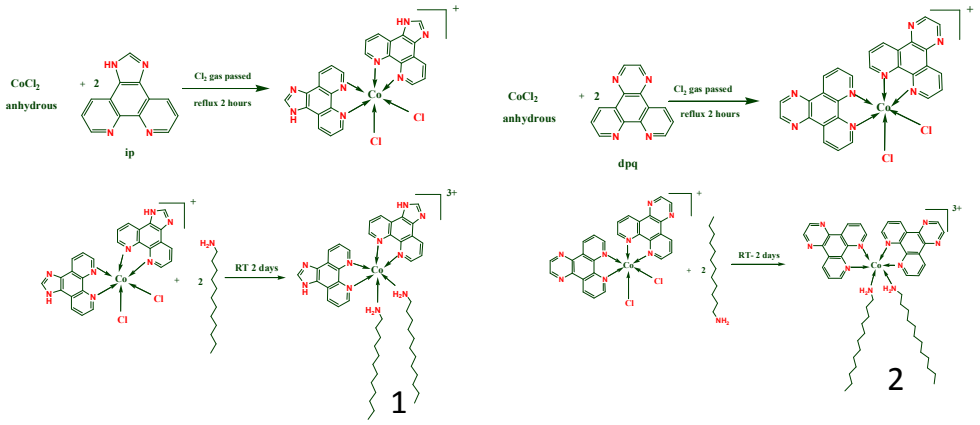

798 Scheme 1. Synthetic route of surfactant complexes **(1)** and **(2)**

799

800

801 Figures

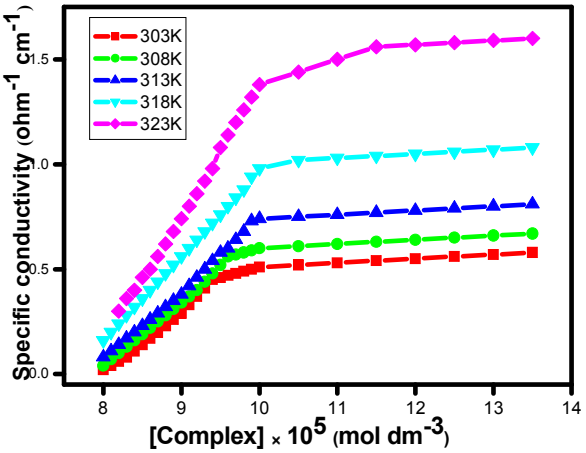

802

Fig. 1

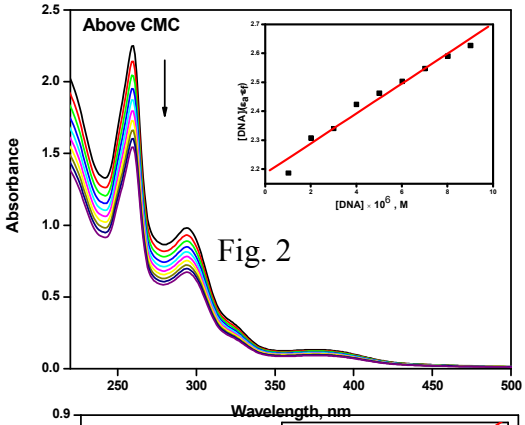

Fig. 2

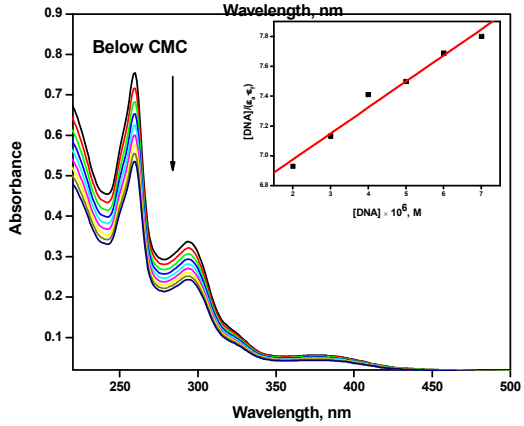

Fig. 3

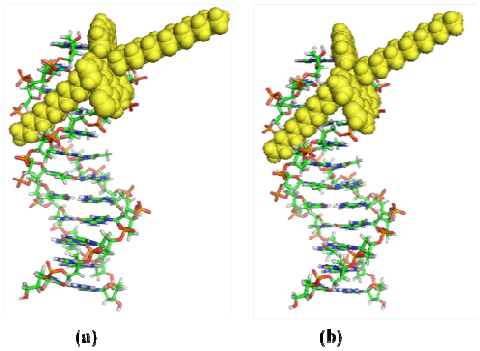

Fig. 4

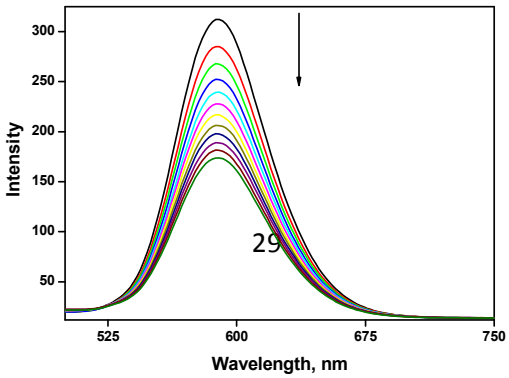

Fig. 5

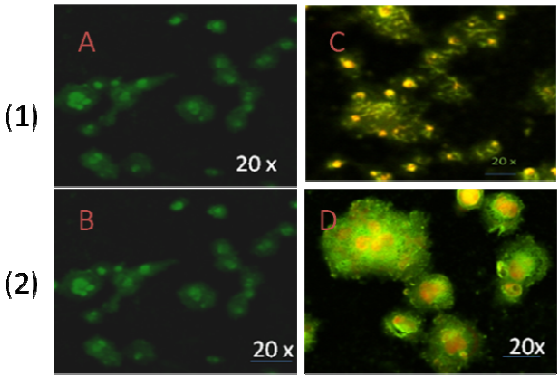

Fig. 6

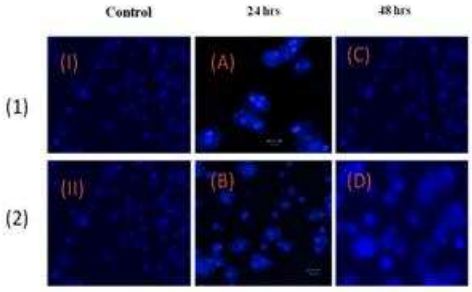

Fig. 7

Tables

Table 1

Temp.	CMC× 10^5	$-\Delta G^0_{mic}$ (kJ mol^{-1})	$-\Delta H^0_{mic}$(kJ mol^{-1})	$T\Delta S^0_{mic}$ (kJ mol^{-1})
303K	9.45	35.0 ± 0.2	11.3 ± 0.3	23.8 ± 0.4
308K	9.64	57.3 ± 0.1	18.8 ± 0.1	38.5 ± 0.1
313K	9.97	78.5 ± 0.1	26.3 ± 0.2	52.2 ± 0.1
318K	10.5	99.9 ± 0.4	34.3 ± 0.1	65.6 ± 0.2
323K	10.89	114.9 ± 0.4	40.3 ± 0.1	74.7 ± 0.2

Table 2

Surfactant Co(III) Complexes	K_b (M^{-1})		Hypochromism		K_{sv} (M^{-1})
	Below CMC	Above cmc			
Complex **(1)**	$(5.7\pm0.2)\times10^5$	$(1.3\pm0.3)\times10^6$	29	31	0.1573
Complex **(2)**	$(2.4\pm0.1)\times10^6$	$(3.1\pm0.2)\times10^6$	34	37	0.1829

Table 3

Energy Levels	Complex **(1)**			Complex **(2)**		
	Co	L1	L2	Co	L1	L2
HOMO-3	0.00	0.00	100.00	0.00	0.00	100.00
HOMO-2	0.43	95.84	3.73	0.00	0.00	100.00
HOMO-1	0.09	40.64	59.27	4.36	3.65	91.99
HOMO	0.05	6.86	93.09	0.91	0.27	98.82
LUMO	0.07	85.15	14.78	53.55	43.02	3.43
LUMO+1	53.15	45.70	1.15	52.04	17.35	30.62
LUMO+2	51.58	17.57	30.85	0.66	96.65	2.69
LUMO+3	0.82	96.35	2.83	1.43	97.58	1.00

Table 4

Surfactant Co(III) Complexes	E_{pc1} (mV)	E_{pa1} (mV)	ΔE_p (mV)	$E_{1/2}$ (mV)	i_{pa}/i_{pc}	E_{pc2} (mV)
Complex **(1)**	-718.5	+13.5	+732.0	-352.5	0.6	-1208.5
Complex **(1)** + DNA	-714.5	+7.5	+721.9	-353.5	0.7	-1202.5
Complex **(2)**	-238.5	+56.5	+295.0	-91.0	1.5	-908.5
Complex **(2)** + DNA	-258.5	+167.5	+426.0	-45.5	1.8	-838.5

Table 5

Complexes	IC_{50} (μm)	
	24 h	48 h
(1)	(6.8± 0.2)	(6.1± 0.2)
(2)	(6.0± 0.2)	(5.0± 0.2)

Graphical Abstract

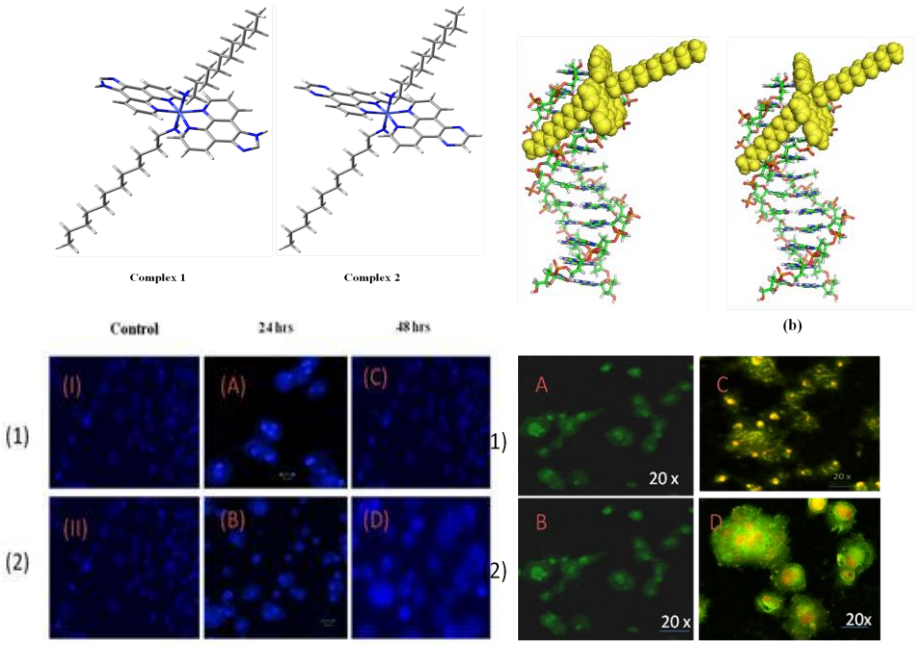

126